Supplementary Material (ESI) for Dalton Transactions

Supporting Information

[18]crown-6 Rotator in Spin-Ladder Compound of m-Aminoanilinium([18]crown-6)[Ni(dmit)$_2$]

Tomoyuki Akutagawa, Daisuke Sato, Qiong Ye, Shin-ichiro Noro, Sadamu Takeda, Takayoshi Nakamura

Full list of all authors in Ref. 19

Frisch, M. J.; Trucks, G. W.; Schlegel, H. B.; Scuseria, G. E.; Robb, M. A.; Cheeseman, J. R.; Zakrzewski, V. G.; Montgomery, J. A., Jr.; Stratmann, R. E.; Burant, J. C.; Dapprich, S.; Millam, J. M.; Daniels, A. D.; Kudin, K. N.; Strain, M. C.; Farkas, O.; Tomasi, J.; Barone, V.; Cossi, M.; Cammi, R.; Mennucci, B.; Pomelli, C.; Adamo, C.; Clifford, S.; Ochterski, J.; Petersson, G. A.; Ayala, P. Y.; Cui, Q.; Morokuma, K.; Malick, D. K.; Rabuck, A. D.; Raghavachari, K.; Foresman, J. B.;. Cioslowski, J.; Ortiz, J. V.; Baboul, A. G.; Stefanov, B. B.; Liu, G.; Liashenko, A.; Piskorz, P.; Komaromi, I.; Gomperts, R.; Martin, R. L.; Fox, D. J.; Keith, T.; Al-Laham, M. A.; Peng, C. Y.; Nanayakkara, A.; Gonzalez, C.; Challacombe, M.; Gill, P. M. W.; Johnson, B.; Chen, W.; Wong, M. W.; Andres, J. L.; Gonzalez, C.; Head-Gordon, M.; Replogle, E. S.; Pople, J. A. *GAUSSIAN 98*; Gaussian, Inc.: Pittsburgh, PA, 1998.

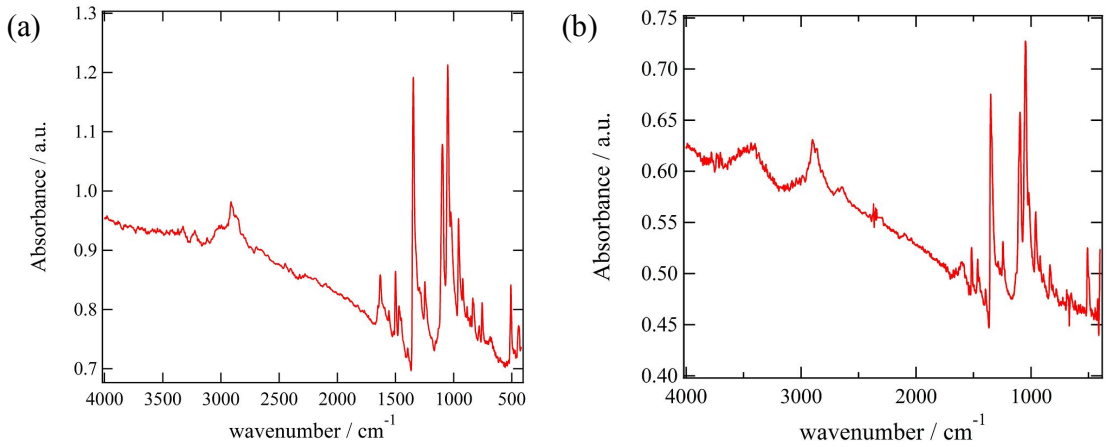

Fig. S1. IR spectra of salts a) **1** and b) **2** in KBr pellets.

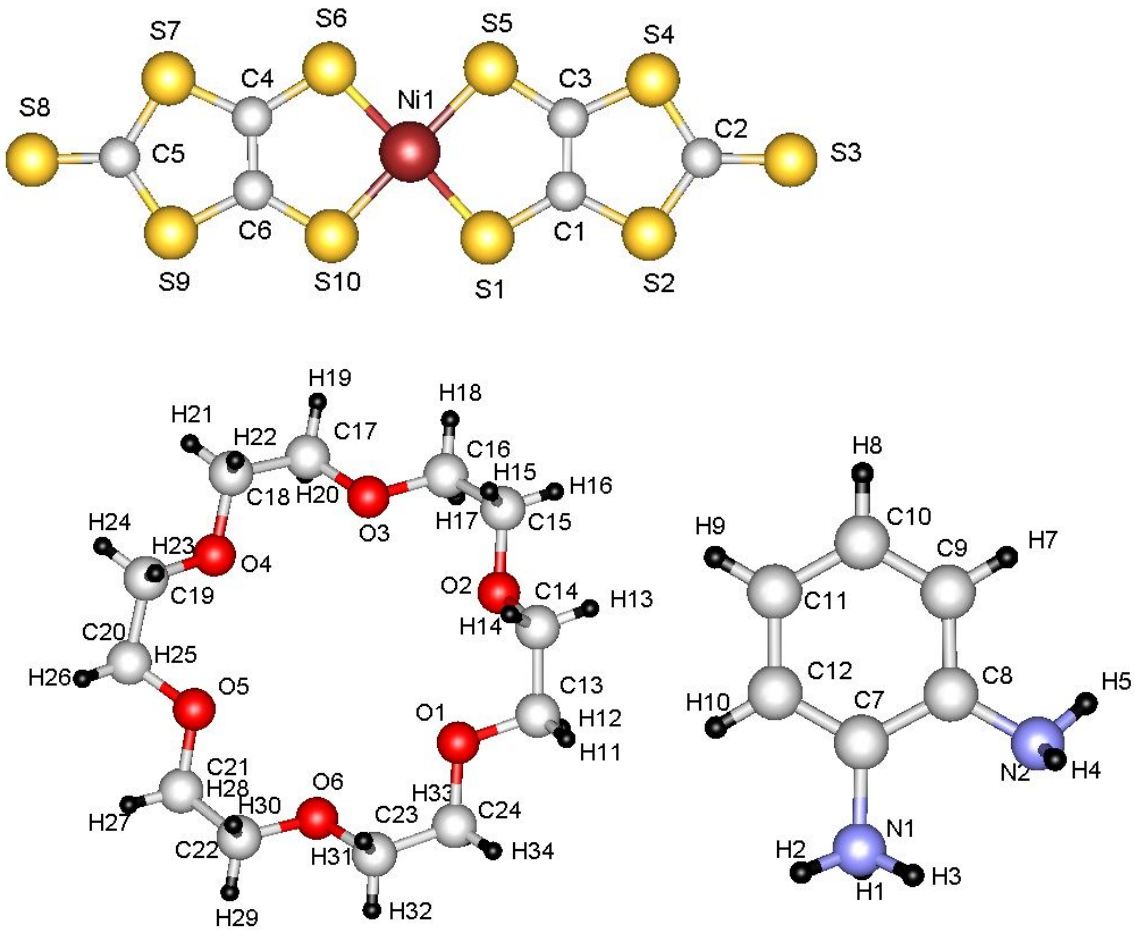

Fig. S2. Atomic numbering scheme of salt **1**.

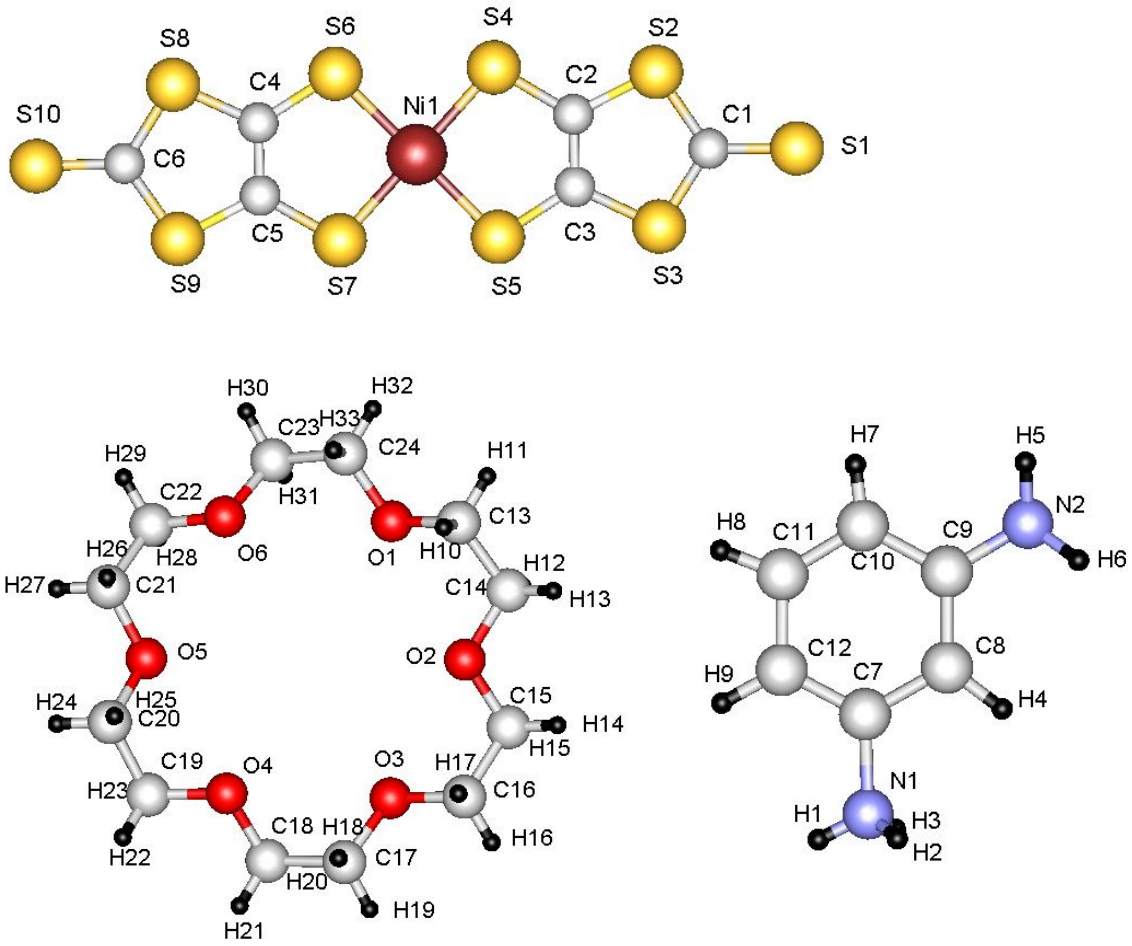

Fig. S3. Atomic numbering scheme of salt **2**.

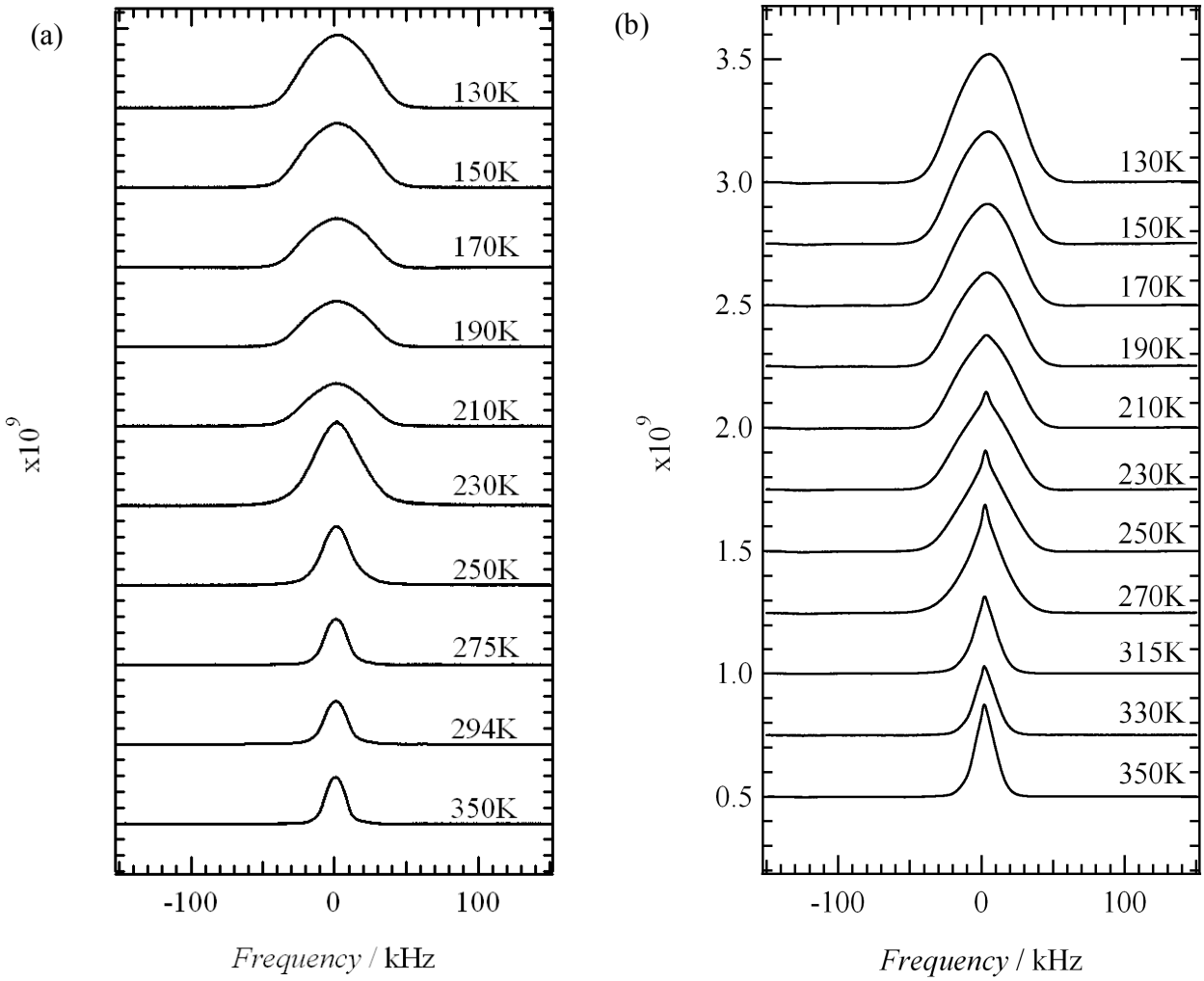

Figure S4. Temperature dependent solid state ^{1}H NMR of salts a) **1** and b) **2**.

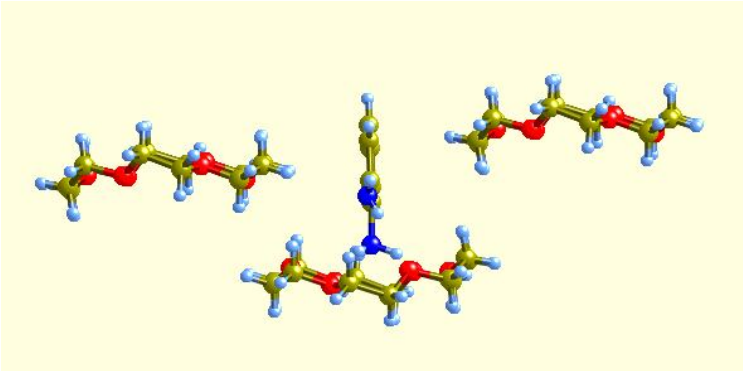

Figure S5. Potential energy calculation of $HOPD^{+}$ cation in $(HOPD^{+})([18]crown\text{-}6)_3$ unit of salt **1**.

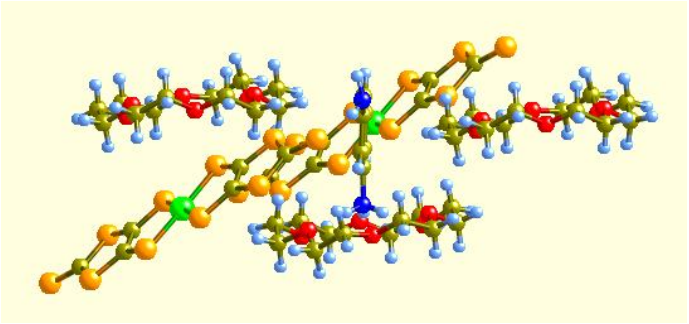

Figure S6. Potential energy calculation of $HMPD^+$ cation in $(HMPD^+)([18]crown\text{-}6)_3[Ni(dmit)_2]_2$ unit of salt **2**.

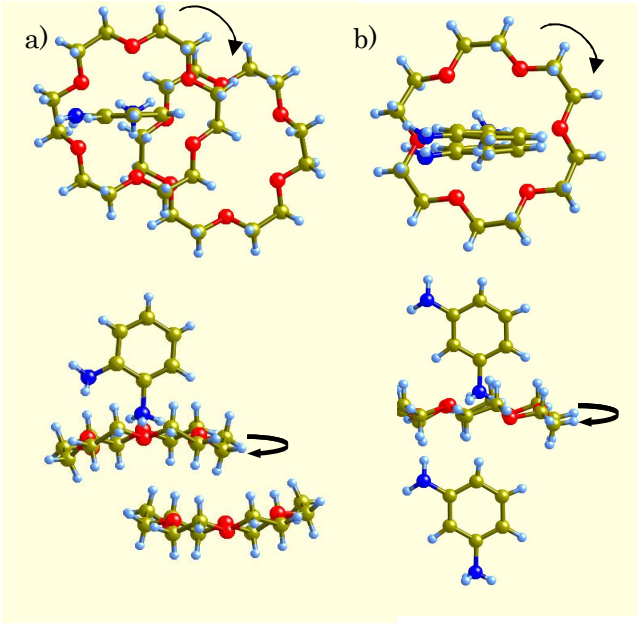

Figure S7. Rotation environment of [18]crown-6 in salts **1** and **2**. a) $(HOPD^+)([18]crown\text{-}6)_2$ in salt **1** and b) $(HMPD^+)_2([18]crown\text{-}6)$ in salt **2**.

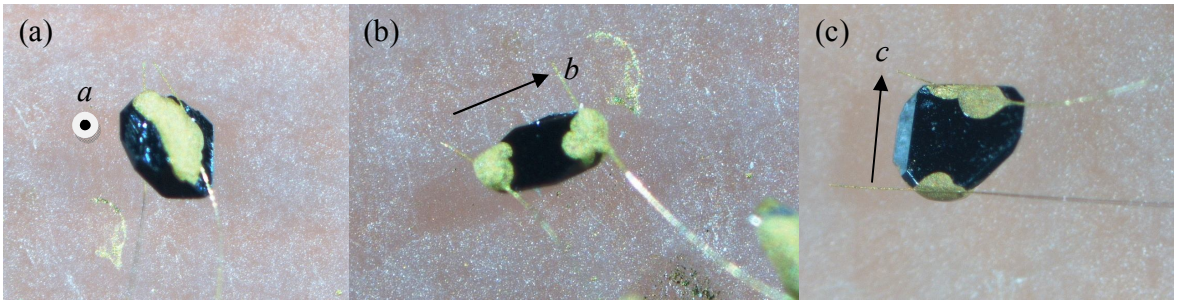

Figure S8. Single crystal for dielectric anisotropy measurements of salt **1**. Au wires were attached along the a) *a*-, b) *b*-, and c) *c*-axis.

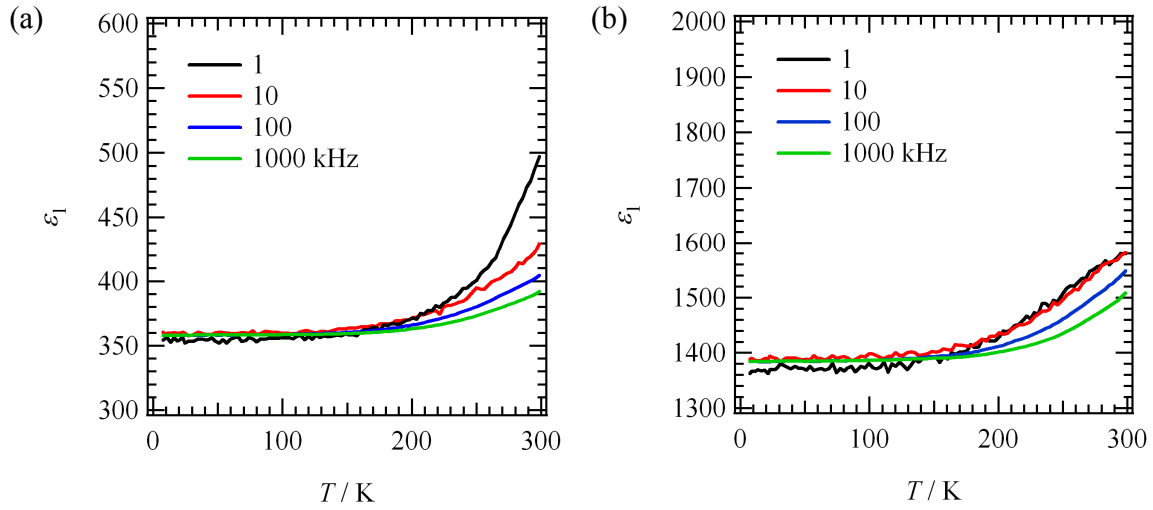

Figure S9. Temperature- and frequency-dependent dielectric constants (ε_1) of salt **1** along the a) *a*- and b) *b*-axes, respectively.

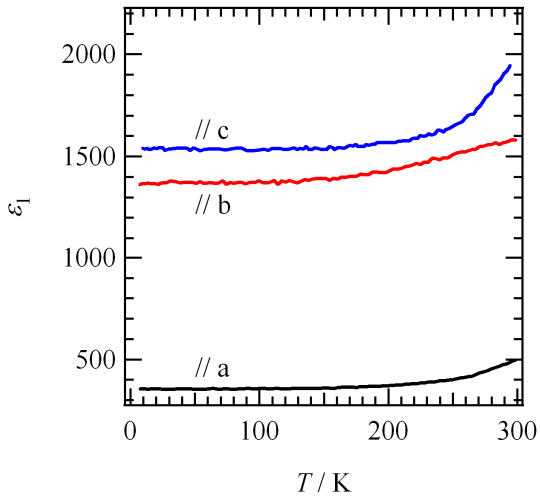

Figure S10 Temperature-dependent dielectric anisotropy of salt **1** along the *a*- (black) and *b*- (red), and *c*-axes (blue), respectively, at the frequency of 10 kHz

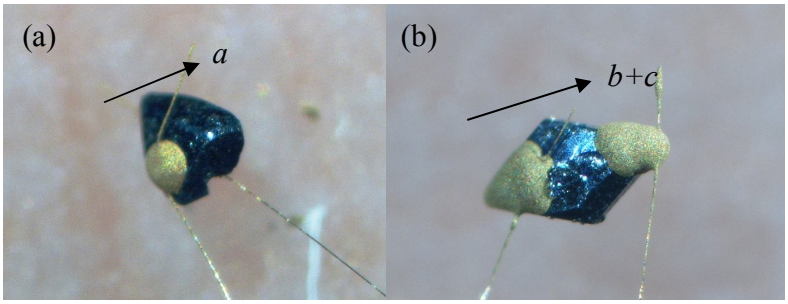

Figure S11. Single crystal for dielectric anisotropy measurements of salt **2**. Au wires were attached along the a) *a*- and b) *b*+*c*-axis.

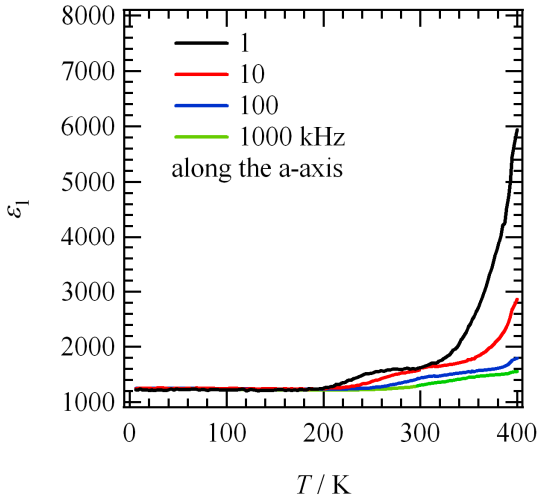

Figure S12. Temperature- and frequency-dependent dielectric constants (ε_1) of salt **2** along the *a*-axis.

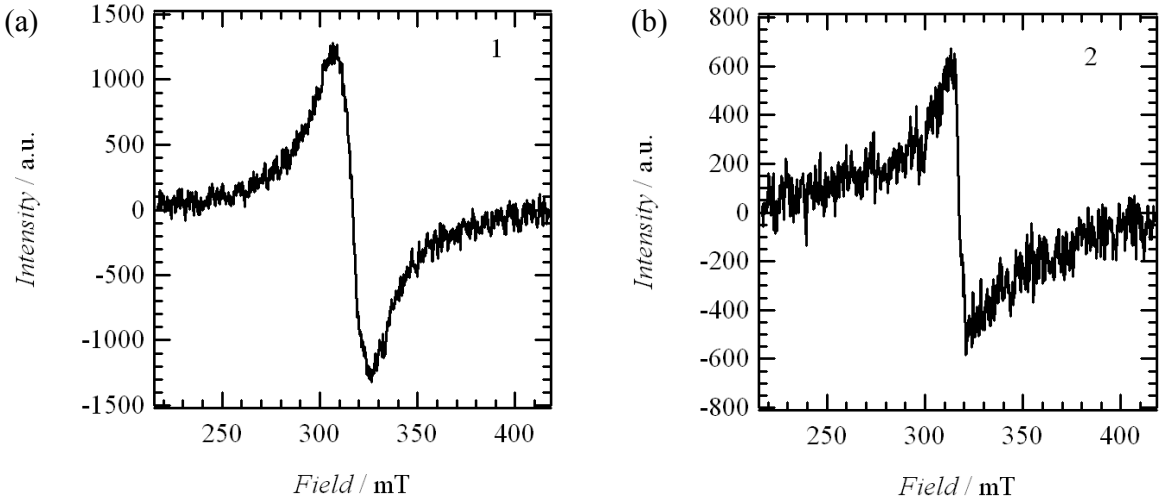

Figure S13. ESR spectra of salts a) **1** and b) **2** at 298 K.

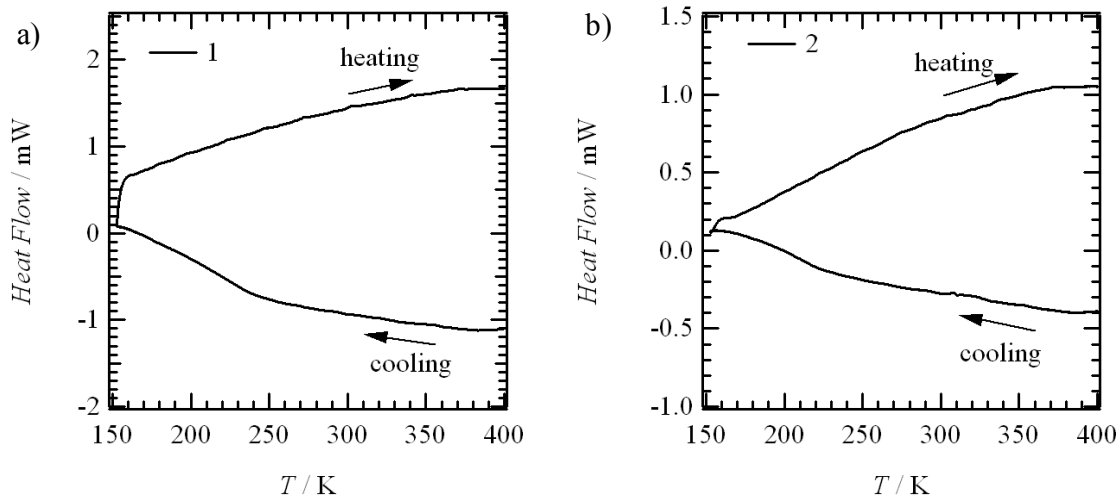

Figure S14. DSC diagram of salts a) **1** and b) **2**.